Available online at www.sciencedirect.com

ScienceDirect

Procedia Structural Integrity 38 (2022) 292–299

Structural Integrity Procedia

www.elsevier.com/locate/procedia

FATIGUE DESIGN 2021, 9th Edition of the International Conference on Fatigue Design

The effect of the environmental conditions on the threshold against fatigue crack propagation

Larissa Duarte[a*], Mauro Madia[a], Uwe Zerbst[a]

[a]*Bundesanstalt für Materialforschung und -prüfung, Unter den Eichen 87, Berlin 12205, Germany*

Abstract

The threshold against fatigue crack propagation (ΔK_{th}) is a crucial parameter for the damage tolerance assessment of engineering components subjected to cyclic loading and it is composed by two distinct components, one intrinsic, dependent on the elastic material properties and the lattice type, and one extrinsic, related to the occurrence of crack closure effects. An important issue is that several factors can influence ΔK_{th} and, in general, the fatigue crack propagation behavior. In this work, the influence of the experimental procedure, air humidity, stress ratio and test frequency on *da/dN-ΔK* data has been investigated. Results are discussed with their potential causes and consequences on the calculations of the residual lifetime.

Keywords: fatigue crack propagation threshold, crack closure effect, experimental procedure, environmental conditions

1. Introduction

The threshold against fatigue crack propagation (ΔK_{th}) is a parameter of paramount importance in the damage tolerance design of engineering components since it defines the stress intensity above which a non-propagating crack starts to propagate. It consists of two components: one intrinsic ($\Delta K_{th,eff}$) and one extrinsic ($\Delta K_{th,op}$). On one hand, $\Delta K_{th,eff}$ seems to be dependent only on material elastic properties, i.e. Young's modulus (E), and lattice type, described by the Burger's vector ($\|\boldsymbol{b}\|$) (see, e.g., Zerbst et. al. (2016)). Analytical solutions such as the ones proposed by Pokluda et. al. (2014), Pippan et. al (2003) and Hertzberg (1995) have been shown to provide

* Corresponding author. Tel.: +49 30 8104-4166.
E-mail address: larissa.duarte@bam.de

2452-3216
10.1016/j.prostr.2022.03.030

Nomenclature

ΔK	cyclic stress intensity factor
ΔK_{th}	fatigue crack propagation threshold
$\Delta K_{th,eff}$	intrinsic component of the fatigue crack propagation threshold
$\Delta K_{th,op}$	extrinsic, closure-related component of the fatigue crack propagation threshold
ΔK_{eff}	cyclic effective crack driving force
$\|\|\boldsymbol{b}\|\|$	Burger's vector
E	Young's modulus
da/dN	fatigue crack propagation rate
CTOD	crack tip opening displacement
R	stress ratio
C	normalized K-gradient
K_{op}	stress intensity factor at crack opening
K_{max}	maximum stress intensity factor during loading cycle
K_{min}	minimum stress intensity factor during loading cycle
PICC	plasticity-induced crack closure
RICC	roughness-induced crack closure
OICC	oxide-induced crack closure
SD	standard deviation

a good approximation of $\Delta K_{th,eff}$ for various materials. On the other hand, $\Delta K_{th,op}$ is related to the so-called crack closure effects at the crack wake. These are the plasticity-induced (PICC), roughness-induced (RICC) and oxide-induced (OICC) as the most important ones. Major influencing factors on crack closure are the crack size (in case of short cracks), the stress ratio (R) and environmental conditions, e.g. air humidity. Since the experimental quantification of crack closure mechanisms is still a problematic task, existing analytical models are only available for PICC, e.g. the one proposed by Newman (1984).

According to Petit et. al. (2003), environmental conditions can affect the crack propagation behavior in two different and opposite ways. If hydrogen embrittlement and anodic metal dissolution, which are detrimental to fatigue properties, take place, higher crack propagation rates (da/dN) are generated and lower threshold values are measured. Otherwise, if oxidation mechanisms associated to oxide-induced crack closure are present, a beneficial effect on fatigue crack growth and the threshold is observed. Because the stress intensity at crack opening (K_{op}) is increased due to the formation of oxide products within the crack, the effective crack driving force leading to crack propagation (ΔK_{eff}) is reduced, so that lower da/dN and higher thresholds are obtained. In this context, temperature, air humidity and stress ratio play a major role. Examples can be found in Suresh et. al. (1981), Suresh et. al. (1983) and Pokorný et. al (2017).

The influence of oxidation on crack growth behavior is mainly (but not only) observed in the so-called threshold and near-threshold regime. There are two reasons for that:

- At this stage the crack propagates at smaller rates, such that more time is available for corrosion reactions to occur;
- The crack tip opening displacement (CTOD) reduces with a reduction in ΔK. In the threshold region, where ΔK approaches smaller values, the crack opening, i.e. CTOD, becomes comparable to the layer thickness of oxide products, i.e. the crack is closed.

Since most of components subjected to cyclic loading are loaded in the threshold region, special attention must be given to the understanding of how oxidation and its influencing parameters affect the crack propagation behavior at lower rates. Therefore, the present work investigates how the absolute air humidity, the stress ratio, the type of experimental procedure and the test frequency influence da/dN-ΔK curves and ΔK_{th} values. The results are discussed together with their potential causes and consequences on the determination of the residual lifetime.

2. Experimental determination of ΔK_{th}

Nowadays, different experimental techniques are applied for the determination of ΔK_{th}, as, e.g., published by Carboni and Regazzi (2011). The methods investigated here are briefly discussed in the following.

2.1. K-decreasing procedure according to ASTM E647 (2015) and ISO 12108 (2018)

By this method, a precrack is generated at a constant ΔK up to a certain size above which the initial notch no longer affects ΔK. Subsequently, ΔK is stepwise reduced at a constant stress ratio (R) and K-gradient (C) until the threshold is reached. C must be chosen in a way that neither plasticity-induced nor oxide-induced crack closure effects influence the results (Zerbst et. al. (2016)). Although both standards provide similar ways for conducting the test, an important difference between them is the *da/dN* limit for which ΔK_{th} is specified: while ASTM suggests $da/dN = 10^{-7}$ mm/cycle, ISO uses $da/dN = 10^{-8}$ mm/cycle. The consequences of this difference and the implication for the calculation of the residual lifetime will be further discussed.

2.2. K_{max} procedure

The K_{max} procedure, briefly mentioned in ASTM E647 (2015), also consists on a stepwise reduction of ΔK after precracking. However, instead of keeping R constant while reducing ΔK, K_{max} is kept constant while increasing K_{min} (and therefore R). At about $R \geq 0.8$, the determined ΔK_{th} is the intrinsic $\Delta K_{th,eff}$.

2.3. Procedures based on compression-precracking

Following the load reduction technique of section 2.1 load history effects resulting from crack closure during precracking can influence *da/dN*-ΔK data and the final ΔK_{th}, and cause non-conservative results. In order to enable the test to be started from a closure-free condition, Pippan (1987) and Tabernig and Pippan (2002) proposed a procedure in which the precrack is generated fully under compression, i.e. both K_{min} and K_{max} are in the compression. This way, *da/dN-ΔK* data are generated with almost no influence of loading history and the crack propagation test can be started from smaller values of ΔK, since it is guaranteed that there will be no crack closure at the beginning of the test.

Depending on how the threshold is finally determined, two different procedures are suggested: CPCA and CPLR. CP stands for compression precracking, CA for constant amplitude and LR for load reduction. Performing CPCA, ΔF is kept constant, so that ΔK increases with increasing crack length, i.e. the threshold is approached coming from lower ΔK. In contrast, in CPLR a similar strategy is adopted as by conventional K-decreasing, the threshold is reached from higher ΔK: it is then reduced at a constant R up to ΔK_{th}. Nevertheless, the test can be started from a lower initial ΔK compared to conventional K-decreasing.

A variant of the CPCA method, here designated as ΔF-constant, has also been applied for the determination of $\Delta K_{th,eff}$ at $R = 0.8$. Since during the whole test a closure-free condition is guaranteed due to the high value of R, precracking has been generated in the same way as in section 2.1.

3. Materials and methods

The material chosen in the present work was the high-strength structural steel S690QL, received as hot-rolled plates with 12 mm thickness. It exhibited a martensitic-bainitic microstructure. Its chemical composition and mechanical properties are provided in Tables 1 and 2. Standard single edge notch bending specimens (SENB), with a length $L = 108$ mm, a width $W = 19$ mm and a thickness $B = 6$ mm, were manufactured with the crack plane parallel to the rolling direction.

Table 1. Chemical composition of the S690QL steel (in % weight)

C	Si	Mn	P	S	N	B	Cr	Cu	Mo	Nb	Ni	Ti	V	Zr	Al	Fe
0,159	0,233	1,15	0,012	< 0,01	0,0095	0,0029	0,408	0,020	0,180	0,036	0,039	< 0,01	< 0,01	0,001	0,082	97,65

Table 2. Mechanical properties of the S690QL steel

Property	Mean	Standard deviation
Elongation at fracture (%)	16,3	0,689
Yield strength (MPa)	810	19,6
Tensile strength (MPa)	825	5,00
E-modulus (GPa)	207	5,16

The fatigue crack propagation tests have been conducted with an 8-point-bending fixture on two different RUMUL resonant fatigue testing machines: a MIKROTRON 654 with a maximum load capacity of 20 kN and a minimum test frequency of about 100 Hz, and a TESTRONIC with a maximum load capacity of 100 kN and a minimum test frequency of about 50 Hz. The crack length has been monitored by means of the direct current potential drop technique (DCPD) with temperature compensation, as proposed by Kruse et. al (2018), and the air humidity and temperature has been recorded during the tests by a Raspberry Pi model B, 4GB Ram.

For the determination of the intrinsic threshold and the investigation on the influence of the experimental procedure on the intrinsic threshold values, the 20 kN Machine was used and four different experimental procedures have been applied: K-decreasing (Section 2.1), CPLR (Section 2.3), ΔF-constant (Section 2.3), at a stress ratio of 0.8, and K_{max} (Section 2.2) at a stress ratio varying from 0.5 at the beginning to 0.8 at the end of the test. To investigate the influence of stress ratio and test frequency on da/dN-ΔK data, specimens were tested by K-decreasing at R = -1 and R = 0.1 on both testing machines. All experiments have been carried out in laboratory air and temperature.

4. Results and discussion

4.1. Determination of $\Delta K_{th,eff}$

In order to illustrate the results obtained at R = 0.8, representative da/dN-ΔK curves of eight specimens are plotted in Fig. 1 (a). The name of each specimen is reported in the legend and the designation ΔK_{th} indicates that threshold and near-threshold data have been recorded. As can be seen, the da/dN-ΔK data exhibit, independently of the procedure applied, very small scatter. The values of $\Delta K_{th,eff}$ are shown in Table 3. It is important to note that, depending on which of the two standards, ASTM or ISO, $\Delta K_{th,eff}$ is based, a difference up to 20 % is found.

Another important observation is that the $\Delta K_{th,eff}$ results were not affected by variations of the absolute humidity measured during the tests (Fig. 1 (b)). This strengthens the hypothesis that E and $\|\boldsymbol{b}\|$ are the only parameters influencing $\Delta K_{th,eff}$. Moreover, the solution proposed Pokluda et. al. (2014) provides a good approximation of $\Delta K_{th,eff}$, whose value lies in between the ISO and ASTM results (see Table 3).

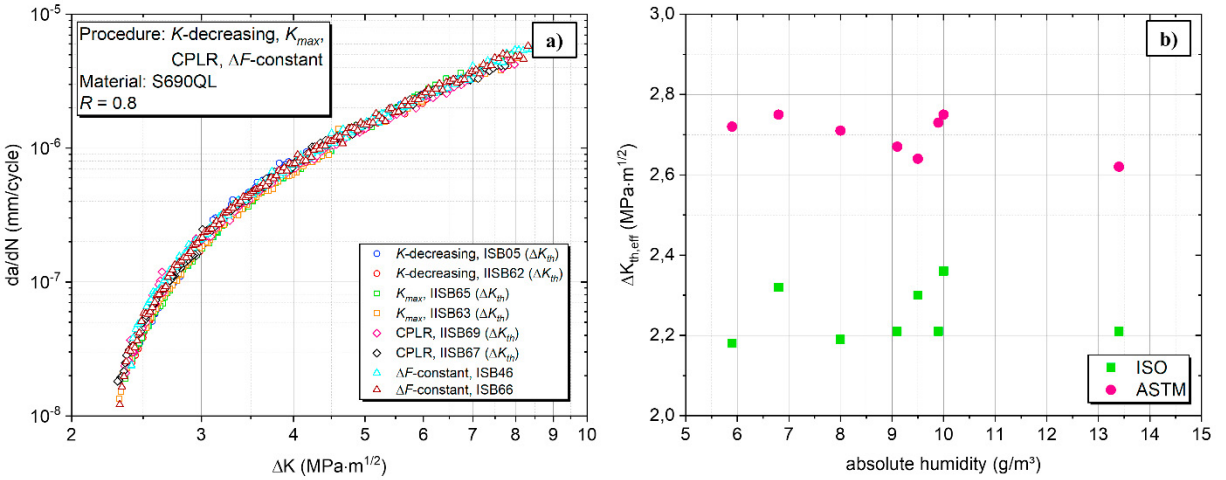

Fig.1. Determination of $\Delta K_{th,eff}$: a) *da/dN-ΔK* curves obtained for different experimental procedures and R = 0.8; b) $\Delta K_{th,eff}$ plotted against measured absolute humidity data.

Table 3. $\Delta K_{th,eff}$ values determined for ASTM and ISO by means of different procedures, and approximated by the solution proposed in Pokluda et. al. (2014)

Procedure	$\Delta K_{th,eff}$ (MPa·m$^{1/2}$) – Mean ± SD	
	ISO	ASTM
K-decreasing	2.23 ± 0.05	2.75 ± 0.03
CPLR	2.18 ± 0.02	2.69 ± 0.02
K_{max}	2.37 ± 0.04	2.80 ± 0.04
ΔF-constant	2.28 ± 0.06	2.65 ± 0.02
E und $\|\|\boldsymbol{b}\|\|$	2.45 ± 0.06	

4.2. Influence of test frequency and stress ratio on da/dN-ΔK data

The influence of the test frequency can be understood as an indirect effect of the oxidation on the crack propagation behavior. If the threshold is approached from higher ΔK (K-decreasing procedure), a lower frequency means that more time is available for the oxidation process, which is a time-dependent phenomenon, and therefore higher thresholds are expected (Table 4). This is exemplified in Fig.2, in which the curve obtained at 50 Hz, turns downward earlier if compared to the curve obtained at 100 Hz. Another important aspect is the non-linear behavior observed around $1 \cdot 10^{-7}$ mm/cycle for the curve on the left which was observed for all specimens tested at 100 Hz, but also only on those specimens. Here, two possible explanations are plausible, which, however, require further investigations:

- The mechanics of fretting corrosion, according to Halliday and Hirst (1956): For higher frequencies some heating is expected at the crack tip and therefore the diffusion of the medium as well as the chemical process of the oxidation are promoted. As the consequence, a larger amount of oxide particles is formed within the crack which, due to mechanical contact between crack faces, enhance the abrasion and removal of material from the surface. When the crack reaches a certain value of the propagation rate (around $1 \cdot 10^{-7}$ mm/cycle) and CTOD, these hard oxide particles tend to roll inside the crack instead of sliding, thus acting like roller bearings. Hence, the coefficient of friction is reduced, and more energy becomes available for the crack to grow. The result is a higher growth rate.
- The inhibition of reverse slip due to oxidation, such as mentioned in Suresh (2003): The formation of oxide products on the crack face, which, as mentioned before, is enhenced at higher frequencies, impedes shear

process during load reversal, what, in turn, means more energy to be available for crack propagation. Thus, although ΔF (and ΔK) are stepwise reduced, an approximately constant crack propagation rate is recorded.

Table 4. ΔK_{th} results obtained through K-decreasing at R = -1 for the frequencies of 100 Hz and 50 Hz.

Frequency	ΔK_{th} (MPa·m$^{1/2}$) – Mean ± SD	
	ISO	ASTM
100 Hz	11.79 ± 1.64	12.30 ± 0.90
50 Hz	12.49 ± 1.63	13.51 ± 1.11

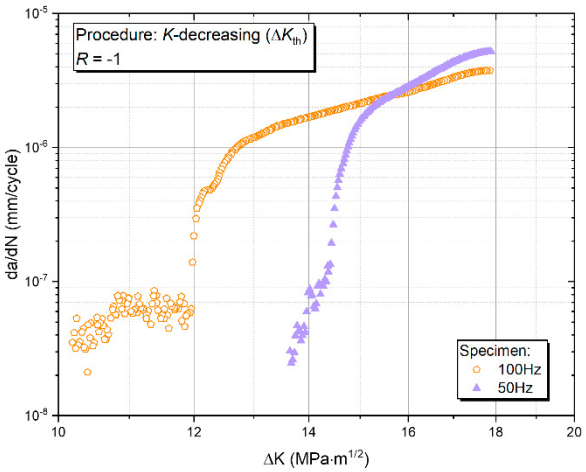

Fig. 2. *da/dN-ΔK* curves recorded for K-decreasing, R = -1 and test frequencies of 100 Hz and 50 Hz. A higher threshold is obtained for 50 Hz, whereas a non-linear behavior is observed for 100 Hz.

Besides the frequency, also the effect of the stress ratio has been investigated. As already mentioned, the effect of R on crack propagation data is often related to the occurrence of crack closure effects in the literature (Suresh et. al. (1981), Suresh et. al. (1983), Pokorný et. al (2017) and Petit et. al. (2003)), which are more pronounced for smaller values of R. This behavior can be observed in Fig.3 (a), in which a higher ΔK_{th} has been recorded for R = -1 than R = 0.1 and R = 0.8. Not surprisingly, the same non-linear effect observed for R = -1 has been noticed for R = 0.1. Moreover, images of the fracture surfaces (Fig. 3 (b)) show a massive formation of oxide products. If the crack length is cross-checked with *da/dN-ΔK* data, one states that the darkest region is generated at crack propagation rates below $2 \cdot 10^{-7}$ mm/cycle.

ΔK_{th} against absolute humidity is plotted in Fig. 4 for all specimens tested at R = -1. Due to both, the frequency effect and the occurrence of non-linear effects, a large scatter band of threshold results has been obtained. At the same time, no correlation between absolute humidity and the crack growth data could be established.

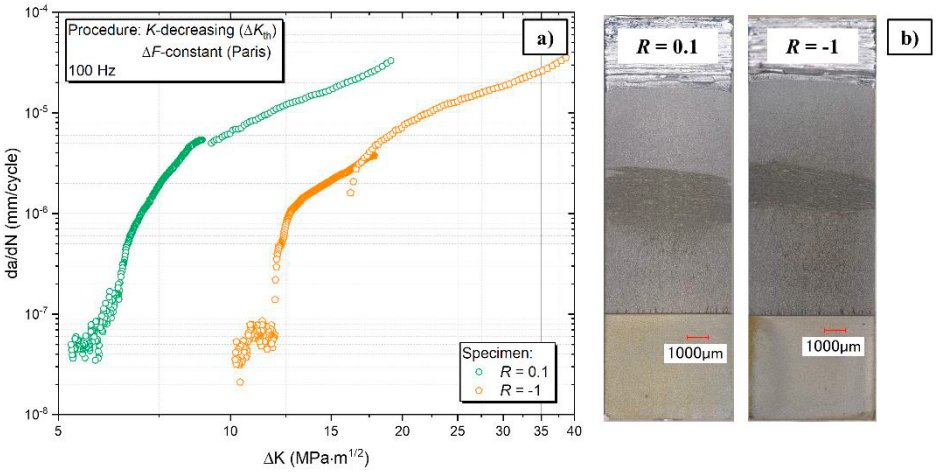

Fig. 3. (a) *da/dN-ΔK* curves recorded for *K*-decreasing and stress ratios of -1 and 0.1. A non-linear curve shape has been observed for both loading conditions; (b) Fracture surfaces indicating a massive oxide formation.

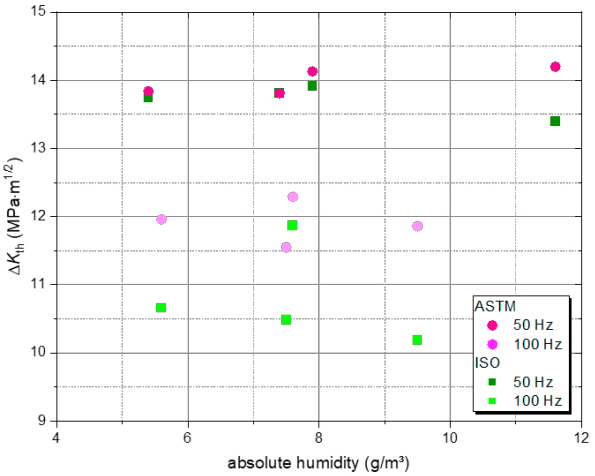

Fig. 4. ΔK_{th} values plotted with their correspondent absolute humidity data. No correlation has been found.

5. Conclusions

The present work evaluated the influence of the testing procedure, the air humidity, the stress ratio and the test frequency on crack propagation data and the fatigue crack propagation threshold. The following conclusions can be drawn:

- The intrinsic threshold values, determined at high stress ratio (R = 0.8), showed a narrow scatter band of data. Absolute air humidity has shown not to have an influence on the results. A critical point is, however, which of the two testing standards, ASTM E647 or ISO 12108 is used for the determination of ΔK_{th}, since a 20 % difference shows up between threshold values.

- Data acquired for R other than 0.8 are strongly dependent on frequency and R. Moreover, corrosion phenomena led to a non-linear behavior at crack rates smaller than $2 \cdot 10^{-7}$ mm/cycle, observed for all specimen tested at R = -1 and 100 Hz. Possible explanations are the mechanisms of fretting corrosion and the inhibition of reverse slip due to the presence of an oxide layer on the surface.

- Concerning the damage tolerant assessment of components, in which a minimal variation of ΔK_{th} can lead to considerable mispredictions, the use of $\Delta K_{th,eff}$ as a material parameter appears to be a promising alternative. It is affected by fewer influencing parameters and can ensure a robust, precise and, in case of doubt, conservative calculation.

Acknowledgements

Mr. Thomas Schwertfeger from the Division 9.4 at BAM is greatly acknowledged for the preparation of the specimens and the assistance during the tests.

Dr. Marcus Klein, Mr. Max Benedikt Geilen and Mr. Josef Schönherr from the MPA-IfW Darmstadt are kindly acknowledged for providing the data about the basic characterization of the S690QL.

This work is part of the research project IFG 20530 N / 1263 " Ermittlung des intrinsischen Schwellenwerts und dessen Validierung als Werkstoffparameter" from the Research Association for steel Application (FOSTA), Düsseldorf, which is supported by the Federal Ministry of Economic Affairs and Energy through the German Federation of Industrial Research Associations (AiF) as part of the program for promoting industrial cooperative research (IGF) on the basis of a decision by the German Bundestag. The project is carried out at BAM Berlin and MPA-IfW Darmstadt.

References

Zerbst, U., Vormwald, M., Pippan, R., Gänser, H.P., Sarrazin-Baudoux, C., Madia, M., 2016. About the fatigue crack propagation threshold of metals as a design criterion – A review. Eng Fract Mech 153, 190-243.

Pokluda, J., Pippan, R., Vojtek, T., Hohenwarter, A., 2014. Near-threshold behavior of shear-mode fatigue cracks in metallic materials. Fat Fract Eng Mat Struct 37, 232-254.

Pippan, R. and Riemelmoser, F.O., 2003. Modelling of fatigue growth: Dislocation models, in: Ritchie, R.O. and Murakami, Y. (eds.): Comprehensive Structural Integrity, vol 4: Cyclic loading and Fracture. Elsevier, 191-207.

Hertzberg, RW., 1995. On the calculation of closure-free fatigue crack propagation data in monolithic metal alloys. Mater Sci Engng A190, 25–32.

Newman Jr J.C., 1984. A crack opening stress equation for fatigue crack growth. Int J Fatigue 24, 131-35.

Petit, J., Henaff, G., Sarrazin-Baudoux, C., 2003. Environmentally assisted fatigue in the gaseous atmosphere. In: Petit, J., Scott, P., editors. Comprehensive structural integrity. Environmentally assisted cracking, vol. 6. Elsevier 2003, 212–80.

Suresh, S., Zamiski, G.F., Ritchie, R.O., 1981. Oxide-induced crack closure: An explanation for near-threshold corrosion fatigue crack growth behavior. Metall Trans A 12A, 1435-43.

Suresh, S., Ritchie, R.O., 1983. On the influence of environment on the load ratio dependence of fatigue thresholds in pressure vessel steel. Eng Fract Mech 18, 785-800.

Pokorný, P., Vojtek, T., Náhlík, L., Hutař, P., 2017. Crack closure in near-threshold fatigue crack propagation in railway axle steel EA4T. Eng Fract Mech 185, 2-19.

Carboni, M., Regazzi, D., 2011. Effect of the experimental technique onto R dependence of ΔKth. Procedia Eng 10, 2937–2942.

ASTM E647-15, 2015. Standard Test Method for Measurement of Fatigue Crack Growth Rates. American Society for Testing and Materials (ASTM), Philadelphia.

ISO 12108, 2018. Metallic materials – Fatigue testing – Fatigue crack growth method. International Organization for Standardization (ISO), Geneva.

Pippan, R., 1987. The growth of short cracks under cyclic compression. Fract Eng Mat Struct 9, 319-328.

Tabernig, B., Pippan, R., 2002. Determination of the length dependence of the threshold for fatigue crack propagation. Eng Fract Mech 69, 899-907.

Kruse, J., Madia, M., Prasad, B., Zerbst, U., 2018. Kompensation von thermoresistivem und thermoelektrischem Effekt bei der experimentellen Bestimmung der zyklischen R-Kurve mit Hilfe der Potentialmethode. Proceedings of the conference Werkstoffprüfung, 6-7 December 2018, Bad Neuenahr, Germany.

Suresh, S., 2003. Fatigue of materials. Cambridge: Cambridge University Press, 2nd ed.